The EMBO Journal Vol.17 No.15 pp.4313–4327, 1998

Structural analysis of the GAP-related domain from neurofibromin and its implications

Klaus Scheffzek[1], Mohammad Reza Ahmadian, Lisa Wiesmüller[2], Wolfgang Kabsch[3], Patricia Stege, Frank Schmitz and Alfred Wittinghofer

Max-Planck-Institut für molekulare Physiologie, Rheinlanddamm 201, 44139 Dortmund and [3]Max-Planck-Institut für medizinische Forschung, Jahnstrasse 29, 69120 Heidelberg, Germany

[2]Present address: Heinrich Pette Institut für experimentelle Virologie an der Universität Hamburg, Martinistrasse 52, 20251 Hamburg, Germany

[1]Corresponding author
e-mail: Klaus.Scheffzek@mpi-dortmund.mpg.de

Neurofibromin is the product of the *NF1* gene, whose alteration is responsible for the pathogenesis of neurofibromatosis type 1 (NF1), one of the most frequent genetic disorders in man. It acts as a GTPase activating protein (GAP) on Ras; based on homology to p120GAP, a segment spanning 250–400 aa and termed GAP-related domain (NF1GRD; 25–40 kDa) has been shown to be responsible for GAP activity and represents the only functionally defined segment of neurofibromin. Missense mutations found in NF1 patients map to NF1GRD, underscoring its importance for pathogenesis. X-ray crystallographic analysis of a proteolytically treated catalytic fragment of NF1GRD comprising residues 1198–1530 (NF1-333) of human neurofibromin reveals NF1GRD as a helical protein that resembles the corresponding fragment derived from p120GAP (GAP-334). A central domain ($NF1_c$) containing all residues conserved among RasGAPs is coupled to an extra domain ($NF1_{ex}$), which despite very limited sequence homology is surprisingly similar to the corresponding part of GAP-334. Numerous point mutations found in NF1 patients or derived from genetic screening protocols can be analysed on the basis of the three-dimensional structural model, which also allows identification of the site where structural changes in a differentially spliced isoform are to be expected. Based on the structure of the complex between Ras and GAP-334 described earlier, a model of the NF1GRD–Ras complex is proposed which is used to discuss the strikingly different properties of the Ras–p120GAP and Ras–neurofibromin interactions.
Keywords: cancer/GTP-hydrolysis/neurofibromatosis/NF1/Ras

Introduction

Neurofibromatosis type 1 (NF1), also termed von Recklinghausen neurofibromatosis, is a common autosomal dominant disease affecting ~1 in 3500 individuals (Riccardi, 1981, 1991; Riccardi and Eichner, 1986). Multiple so-called 'café au lait' spots, Lish nodules of the iris, and neurofibromas, benign cutaneous tumours, are hallmarks of the disease with important diagnostic relevance. While several manifestations are benign in character some of them involve a significant risk of developing malignant or fatal traits, such as plexiform lesions or optic glioma (Gutmann and Collins, 1993). Therefore, NF1 has been grouped together with familial cancer syndromes (Bader, 1986).

The *NF1* gene has been identified to code for a large transcript that is disrupted or mutated in patients affected with NF1 (Cawthon *et al*., 1990; Viskochil *et al*., 1990; Wallace *et al*., 1990). Since the gene appeared to be inactivated in tumours it has been postulated to act as a tumour suppressor (Ponder, 1990; Stanbridge, 1990). In spite of conflicting genetic results, experimental evidence accumulated during the past few years indicate that loss of heterozygosity (LOH) precedes fibrosarcomas and other lesions, with a somatic mutation following an inherited mutant allele (Serra *et al*., 1997).

NF1 codes for a protein comprising 2818 amino acids (Marchuk *et al*., 1991) termed neurofibromin (~280 kDa) that is found in the particulate fraction bound to a very large protein (DeClue *et al*., 1991). Analysis of the predicted protein sequence revealed homology between a segment spanning 250 amino acids with high and an additional 150 amino acids with lower homology to Ras-specific GTPase activating proteins (Xu *et al*., 1990a) such as p120GAP (Trahey and McCormick, 1987) and its yeast homologues IRA1 and IRA2 (Tanaka *et al*., 1990a,b, 1991). Biochemical analyses and functional complementation tests in yeast established this segment as a functional GAP-related domain (NF1GRD) that is able to stimulate GTP-hydrolysis on normal but not oncogenic Ras (Ballester *et al*., 1990; Martin *et al*., 1990; Xu *et al*., 1990b), thus linking neurofibromatosis to the regulation of the Ras–MAP kinase pathway and its activation by oncogenes (Lowy and Willumsen, 1993). It has indeed been found that Ras is mostly in the GTP-bound form in cell lines established from malignant tumours without functional neurofibromin (Basu *et al*., 1992; DeClue *et al*., 1992; Guha *et al*., 1996), suggesting that neurofibromin is a major regulator of Ras in the parental cells due to its GAP activity. Further studies indicate that another mechanism of NF1-mediated tumour suppression is possibly independent of its GAP activity (Nakafuku *et al*., 1993; Johnson *et al*., 1994; Griesser *et al*., 1995). Four differentially spliced isoforms have been detected so far (Gutmann *et al*., 1995), one of which, the type II transcript, is characterized by a 21 amino acids insertion within the GAP-related domain (GRD; Nishi *et al*., 1991; Suzuki *et al*., 1991; Andersen *et al*., 1993). Somatic mutations in

NF1 have been shown to map to the GRD and affect the interaction with Ras (Li *et al*., 1992; Purandare *et al*., 1994; Upadhyaya *et al*., 1997; Klose *et al*., 1998), underscoring the importance of this part of the protein for proper neurofibromin function. Neurofibromin has been shown to associate with microtubules (Gregory *et al*., 1993) thus linking its function to aspects of structural reorganization of the cytoskeleton. It binds tubulin and the binding region presumably overlaps with NF1GRD since tubulin inhibits GAP activity (Bollag *et al*., 1993). The fundamental physiological importance of neurofibromin is underscored by the observation that mice with a targeted disruption of the neurofibromin locus are embryonically lethal and show abnormalities of neural crest-derived tissues (Brannan *et al*., 1994; Jacks *et al*., 1994).

We have previously determined the structure of GAP-334 (Scheffzek *et al*., 1996), the NF1GRD homologue in p120GAP, and of its complex with Ras (Scheffzek *et al*., 1997). Together with biochemical analyses (Mittal *et al*., 1996; Ahmadian *et al*., 1997b) this enabled us to characterize the Ras–RasGAP interaction and to elucidate the mechanism of GTPase activation. In order to address the specific issues underlying neurofibromin function, we report here the crystal structure of NF1GRD, determined from a proteolytically treated fragment comprising residues 1198–1530 (NF1-333). Significant but limited homology with GAP-334 suggested structural similarity but also differences that might account for the strikingly different biochemical behaviour of the two proteins: (i) on a structural level, the minimal domain with full catalytic activity obtainable by limited proteolysis or recombinant expression is 270 residues for p120GAP, compared with 230 for neurofibromin (Ahmadian *et al*., 1996). (ii) For neurofibromin, a fragment of 91 residues has been defined to retain some catalytic activity and yet does not contain residues thought to be critical for catalysis, and an even smaller fragment with anti-oncogenic activity from the C-terminus of the catalytic fragment has been reported (Nur-E-Kamal *et al*., 1993; Fridman *et al*., 1994). The putative catalytic activity of these fragments could not be reconciled with the structure of GAP-334 or of its complex with Ras, raising the possibility of significant deviations in the NF1GRD–Ras interaction pattern. (iii) The affinity of neurofibromin for Ras-GTP is 50- to 100-fold higher than that of p120GAP, and the kinetics of association and dissociation are much faster for the latter (Eccleston *et al*., 1993; Ahmadian *et al*., 1997a). (iv) Although the catalytic activity of both GAPs is generally sensitive to the presence of detergents, specific inhibition of neurofibromin can be obtained by applying selective compounds such as dodecyl maltoside (Bollag and McCormick, 1991).

On the basis of our structural model we analyse these features together with mutations found in NF1 patients or derived from mutational studies. In addition, we discuss aspects of NF1–tubulin interaction and, on the basis of the Ras–RasGAP complex, propose a Ras–NF1GRD complex model that should be an approximation of the transition state of the GTPase reaction.

Results and discussion

Structure determination and model quality

The structure was determined by X-ray crystallographic analysis of crystals obtained from proteolytically treated NF1-333 (described in Materials and methods). Since attempts to solve the structure by molecular replacement using the coordinates of GAP-334 (protein data bank accession code 1WER) as a search model were not successful, we used the Multiple Isomorphous Replacement (MIR) method. Using mercury and platinum derivatives we obtained a heavy atom model suitable for initial phase determination with a data set of 2.5 Å resolution, collected from six untreated crystals on the synchrotron beam line X11 at EMBL (c/o DESY; Hamburg, Germany), as native reference (Table I; Materials and methods). The initial electron density map (Figure 1A) was readily interpretable and could accommodate a C_α-model corresponding to the central domain (GAP_c) of GAP-334 (Scheffzek *et al*., 1996), which served as a guide during subsequent model building and refinement. Remaining density within the asymmetric unit could be explained in part by N-terminal extension of this model up to residue 1206. Two further helices turned out to represent segments derived from the C-terminal region of NF1-333 (Figure 1A). Analysis of dissolved crystals or of the protein solution used for crystallization by polyacrylamide gel electrophoresis revealed two major components to be present in the crystals. N-terminal sequencing along with mass spectroscopy suggested that protease treatment of NF1-333 had nicked the polypeptide chain close to the position of Ser1474. The structural integrity of NF1-333 appears to remain basically unaffected by protease digestion. The observed crystal packing is consistent with an NF1GRD protein cleaved in the segment containing the proteinase K cleavage site, and would not be compatible with uncleaved NF1-333 in the asymmetric unit.

A high degree of mobility appears to be characteristic of the NF1-333 in our crystals with extensive regions remaining without well defined electron density. In successive rounds of interactive model building (program 'O'; Jones *et al*., 1991 and refinement (program X-PLOR; Bruenger, 1991), residues showing sufficient electron density were incorporated into the model, that presently contains 260 residues of NF1-333 defining regions 1206–1304, 1331–1403, 1412–1463, 1485–1503 and 1514–1530, with interspacing segments predominantly ill-defined in the electron density map. In the present model, ~30 residues were built as alanine or glycine because of unclear side-chain density. A segment of the final $2F_o–F_c$ map is shown in Figure 1B. Refinement statistics and model quality are summarized in Table II, including those for the GAP-334 model which had not been completed at the time of its publication (Scheffzek *et al*., 1996). The current *R*-factor is 27% (R_{free} = 37%), which is comparatively high and at least in part reflects residual electron density that could not be explained in terms of ordered polypeptide chains. For the following reasons we are very confident that the current NF1GRD model is largely correct: (i) we used the MIR method for structure determination, thus our initial phases are unbiased by the GAP model that only served as a guide for model building; (ii) coordinates of heavy atom sites are consistent with the mercury compound binding to cysteines; (iii) a loop which by sequence comparison contains three amino acids less than the corresponding stretch in GAP-334 is correspondingly shorter in NF1-333 (Figure 1C; see below). Thus, together

Table I. Structure determination

Crystal: a = 88.2 Å; b = 58.3 Å; c = 74.8 Å; $\alpha = \gamma = 90°$, $\beta = 118.1°$; spacegroup C2

	Native	CH_3HgCl[a]	CH_3HgCl/K_2PtCl_4[b]	ICH_2COOH/K_2PtCl_4[c]
Data collection:				
resolution (Å)	2.5	3	3.5	3
No. obs. reflections	50 100	14 694	13 533	18 658
No. uniq. reflections	11 665	6191	4019	6262
completeness (%)	99.8	91.6	96.5	92.6
R_{sym}[d] (%)	7.3	5.4	6.3	4.9
R_F[e] (%)	–	33.1	38.3	26.3
MIR-analysis:				
resolution (Å)	15–2.5	15–3	15–3.5	15–3
No. sites	–	3	5	3
R_C[f]	–	0.5	0.43	0.76
F_H/E[g]	–	1.8	2.1	0.9
<m>[h]	0.5			

[a]1 mM, 12 h; [b]1 mM, 7 h/+0.1 mM, 15 h; [c]2 mM, 24 h/0.2 mM, 23 h.

[d]$R_{sym} = \sum_h \sum_i \left| I_{hi} - I_h \right| / \sum_{hi} I_{hi}$, where I_{hi} is the scaled intensity of the ith symmetry-related observation of reflection h, and I_h is the mean value.

[e]$R_F = 2 \sum_h \left| F_{PH} - F_P \right| / \sum_h \left| F_{PH} + F_P \right|$, where F_{PH} and F_P are the derivative and native structure amplitudes.

[f]$R_C = \sum_h \left| P_{PH,obs} - F_{PH,calc} \right| / \sum_h \left| F_{PH,obs} - F_P \right|$.

[g]$F_H/E = \sqrt{f_H^2 / \sum (F_{PH,obs} - F_{PH,calc})^2}$, where f_H^2 are the heavy atom scattering factors.

[h]<m> = mean figure of merit.

with the results of structure refinement, several lines of evidence indicate that our structure determination presents a valid model of NF1GRD, suitable for analysis of various mutations associated with NF1 and with the structure of the Ras–GAP-334 complex at hand to discuss effects on the interaction with Ras.

Overall structure

The purely helical protein is similar in structure to GAP-334 with a central domain ($NF1_c$; segments 1253–1304, 1331–1403 and 1412–1463) containing the conserved residues and an extra domain ($NF1_{ex}$) that comprises segments 1206–1252, 1485–1503 and 1514–1530 (Figure 2A and C). For graphic representation and clarity the regions missing from our NF1GRD model were complemented by the corresponding segments of the GAP-334 model where they are mostly well-defined. The two structures superimpose (Figure 2B) with an r.m.s.d. value of 1.83 Å when comparing the positions of 243 corresponding C_α-atoms using program 'O' (Jones *et al*., 1991). The largest differences are seen in the extra domain where helix $\alpha 1_{ex}$ appears to be shifted by ~3 Å in comparison with the corresponding helix in GAP_{ex}. The central domain coincides with a minimal catalytic fragment of neurofibromin with full GAP activity, which was originally obtained by proteolysis and can be expressed as a recombinant fusion protein and cleaved (Ahmadian *et al*., 1996). Interestingly, the corresponding fragment of p120GAP could not be expressed in *Escherichia coli* as a soluble protein. This suggests that despite close similarities in the primary sequence, subtle differences exist in the interaction patterns between the extra and the central domain in these two GAPs, and might influence flexibility and/or exposure of hydrophobic residues. With regard to the absence of sequence homology within the extra domains of GAP-334 and NF1GRD, and to the fact that they are not involved in the interaction with Ras-GTP, their structures are surprisingly similar. This suggests a conserved function for this part of the proteins, possibly serving structural 'assistance' for the central catalytic GAP modules. A detailed analysis of this issue will have to await the structure determination of other RasGAPs, which show no or very limited sequence homology outside the central catalytic domain (Figure 2C).

Regions of high mobility predominantly include segments connecting helices as indicated in Figure 2A and B. As extrapolated from the GAP-334 model, an extended chain linking the C-terminal end of $NF1_c$ to $NF1_{ex}$ contains the proteinase K cleavage site; since the corresponding region is flexible in GAP-334 as well, it is unlikely that this is due to cleavage in NF1-333: rather, flexibility makes this region more accessible to the protease. It is possible that the extensive mobility which is also reflected in the high Wilson B-factor (~50 $Å^2$) provides an explanation why poor diffraction quality is common in most of our previously obtained crystals containing fragments of NF1GRD.

The Ras-binding groove

Given the similarity of GAP-334 and NF1-333, we use corresponding structural annotations and can identify the Ras-binding site as the groove in the surface of $NF1_c$, which is bordered mainly by the finger loop ($L1_c$) along with part of helix $\alpha 2_c$ and by the variable loop ($L6_c$; Figure 2A and C) (Scheffzek *et al*., 1997). Helix $\alpha 6_c$ is less distorted than in GAP_c with only Phe1392, next to the FLR-finger print motif of RasGAPs, interrupting the ideal helix geometry. Various hydrophobic and polar residues cover the floor of the groove, comprising conserved/invariant residues and amino acids that are different

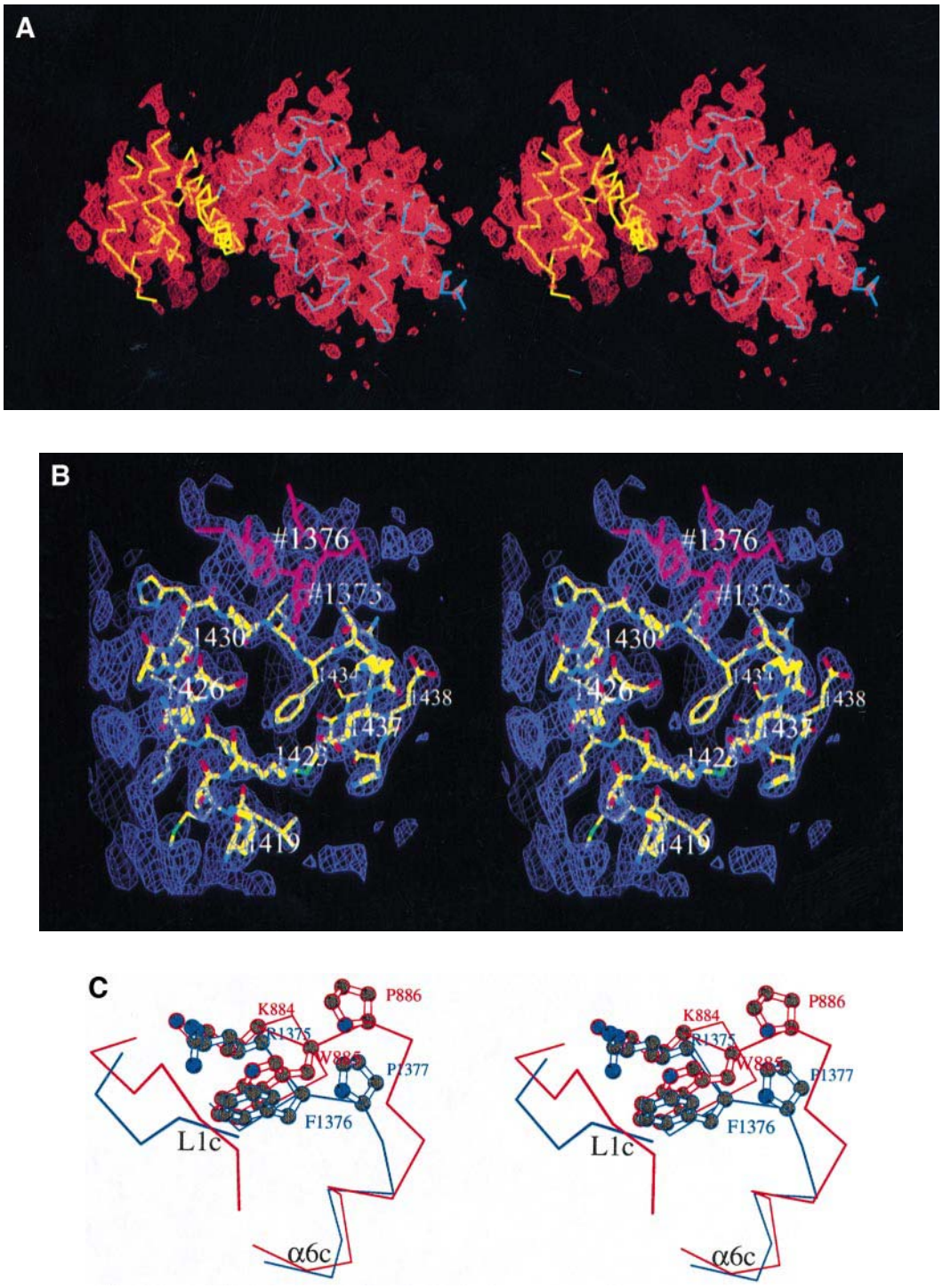

Fig. 1. Aspects of structure determination (stereo views). (**A**) Experimental MIR map, (contoured at 20% of the maximum) calculated with phases derived from the heavy atom model. The C_α-traces of the central (blue) and extra domain (yellow) are included. (**B**) Segment of the $2F_o–F_c$ map (contoured at 1.2 σ) covering the C-terminal half of helix $\alpha7_c$ and the variable loop ($L6_c$) after structure refinement with the model included. A segment of a neighbouring molecule covering residues 1373–1377 [see (C)] is shown in pink. (**C**) Section comparing NF1GRD (blue) and GAP-334 (red) in the region of the loop preceding $\alpha6_c$, showing a three residue insertion in GAP-334 (see Figure 2B). Arginine 1375 contacts the N-terminal region of the finger loop. The corresponding situation is found for Lys884 in GAP-334.

from their GAP-334 counterparts. The most prominent deviation is seen in position 1419 where a lysine protrudes into the groove, corresponding to an isoleucine (Ile931) in GAP-334 (see below). p120GAP and NF1GRD are inhibited by a large number of lipids, some of which act differentially (Bollag and McCormick, 1991; Golubic *et al*., 1991; Serth *et al*., 1991; Tsai *et al*., 1991). Using appropriate concentrations of arachidonate, phosphatidate and phosphatidylinositol-3,4-bisphosphate, NF1GRD can be inhibited without disturbing p120GAP activity.

Table II. Refinement statistics

Refinement	NF1-333	GAP-334[a]
Resolution (Å)	30–2.5	5–1.6
No. reflections	10 926 (F >2 s)	40 803
R_{cryst}[b] (%)	27	22.1
R_{free}[c] (%)	37	27.1
<B> (Å^2)	46.8	26.1
r.m.s. bond length (Å)	0.008	0.007
r.m.s. bond angle (°)	1.2	0.9

[a]Refinement statistics for the final model as released in the PDB.

[b]$R_{cryst} = \sum_h \left| F_{oh} - F_{ch} \right| / \sum_h F_{oh}$, where F_{oh} and F_{ch} are the observed and calculated structure factor amplitudes for reflection *h*.

[c]*R*-factor calculated for 10% randomly chosen reflections not included in the refinement.

Likewise, dodecyl maltoside has been used to distinguish between neurofibromin and p120GAP activity in crude cell extracts (Bollag and McCormick, 1991). It is probable that the amino acid composition in the groove region contributes significantly to these differential properties. The structure suggests that these properties arise from a few residues in this region. Mutational analysis would be a powerful tool to address this question in more detail.

The finger loop appears to be more flexible than in GAP-334; as in GAP-334 the stretch preceding the finger arginine (Arg1276) is stabilized by a phenylalanine and a leucine participating in a hydrophobic core. The orientation of the loop is stabilized by the FLR-arginine (Arg1391), the structural and functional equivalent of Arg903 in GAP-334. The N-terminal region of the finger loop appears to be stabilized by Arg1375 which is packed against the neighbouring Phe1376 and belongs to the loop connecting helices $\alpha5_c$ and $\alpha6_c$. In GAP-334 an equivalent situation can be observed, where Lys884, packed against Trp885, interacts with the N-terminal part of the finger loop. The loop carrying Lys884 contains three residues more than the NF1GRD counterpart and therefore appears as a 'bulge' in a structural overlay (Figure 1C). The variable loop is in a similar conformation to that which it adopts in GAP-334 with Ala948 as an extra amino acid in GAP-334, in support of the idea that this loop is of variable length in RasGAPs (Scheffzek *et al*., 1997).

The minimum catalytic domain, a controversy?

Conflicting evidence to localize the minimal fragment of NF1GRD able to stimulate Ras-mediated GTP-hydrolysis has been reported. Originally, a 483 residue fragment of neurofibromin was classified as a GAP-related domain (Martin *et al*., 1990), and was later shown to have similar enzymatic properties as full-length neurofibromin (Bollag and McCormick, 1993). In analogy to p120GAP where the 334 C-terminal amino acids were shown to be sufficient for GAP activity (Marshall *et al*., 1989), NF1-333, homologous in sequence to GAP-334, and similar constructs were shown to be fully active and were extensively analysed kinetically and by equilibrium methods (Wiesmüller and Wittinghofer, 1992; Brownbridge *et al*., 1993; Eccleston *et al*., 1993; Nixon *et al*., 1995; Ahmadian *et al*., 1997a). Finally, proteolysis experiments and recombinant expression studies showed a 230 residue fragment (Asp1248 to Phe1477; Figure 2C) to retain full catalytic activity (Ahmadian *et al*., 1996). From these experiments together with the crystal structures of GAP-334 (Scheffzek *et al*., 1996) and NF1GRD (this paper) we conclude that the central domains indeed represent minimum RasGAP-modules.

Using a deletion cloning approach a fragment of 91 amino acids (NF91; 1441–1531; Figure 2C) was identified to reverse the malignant phenotype induced by v-H-Ras, and to carry GAP activity, although 20-fold lower than NF1GRD (Nur-E-Kamal *et al*., 1993). In the structure this fragment would start at the C-terminal end of the variable loop and comprise helices $\alpha8_c$, $\alpha4_{ex}$-$\alpha6_{ex}$ (Figures 2C and 3), and thus be located completely outside the region that has been found to interact with Ras in the Ras–RasGAP complex (Scheffzek *et al*., 1997) and contains none of the critical residues of RasGAPs. One would have to postulate that the GAP activity reported for the NF91 fragment or its smaller relative NF78 (Fridmann *et al*., 1994) occurs by a mechanism that uses a protein–protein interface different from that described for the Ras–RasGAP complex. Site-directed mutagenesis of Arg1441 which is in a region reported to be critical for the function of this fragment might be a useful approach to address this issue.

Patient mutations and structure–function studies

Locations of mutations discussed in this section are summarized in the model shown in Figure 3. A variety of alterations in the *NF1* gene have been found in tissues from NF1 patients, with no apparent hot-spot region (Shen *et al*., 1996). Very large deletions of up to 190 kb, and nonsense mutations all lead to truncation of the protein product, whereas small deletions induce frameshifts. A limited number of missense mutations has been described, 20% of which are found in the catalytic and 1% in the extra domain of NF1GRD, some of which affect the GAP-activity (Figures 2A and C, and 3) (Li *et al*., 1992; Purandare *et al*., 1994; Upadhyaya *et al*., 1997; Klose *et al*., 1998; P.Nürnberg, unpublished).

Lysine 1423 appears to be the most frequently altered residue and has been found mutated to glutamate or glutamine in neurofibromas as well as in solid tumours not associated with neurofibromatosis, which reportedly inhibits the GAP activity (Li *et al*., 1992; Upadhyaya *et al*., 1997). Extensive analyses of this residue by site-directed mutagenesis have tested every natural amino acid substitution along with biochemical/biological characterization of the mutant proteins (Poullet *et al*., 1994). These studies showed that the original wild-type residue lysine in position 1423 is the only amino acid that results in a functional protein, and suggest decreased Ras affinity as the major effect of Lys1423 mutations (Poullet *et al*., 1994), in line with earlier data on Lys1423→Ser by Gutmann *et al*. (1993). In the structure, Lys1423 is located on helix $\alpha7_c$ from which it protrudes into the surface groove to interact with Glu1437 (Figures 1B and 4). As an analogous interaction is weak in isolated GAP-334 (Scheffzek *et al*., 1996) but very prominent in complex with Ras (Scheffzek *et al*., 1997), it appears to be additionally stabilized during the interaction with the Ras target; it is conceivable that charge inversion in this region

(as in the mutation Lys1423→Glu) not only disrupts a favourable internal interaction but might also contribute to the accumulation of negative charges in the interface region which is unfavourable for the mostly acidic effector region of Ras entering the surface groove. Correspondingly, the replacement by arginine has been scored as the least, and by glutamate as the most severe mutation of Lys1423 (Poullet *et al*., 1994). Involvement of Lys1423 in an intramolecular polar interaction was in fact proposed by Wiesmüller and Wittinghofer (1992) on the basis of its mutation to methionine that produced a thermally unstable protein.

In a yeast genetic screen, Poullet *et al*. (1994) identified mutations of Phe1434 to serine or leucine as second site suppressors of certain Lys1423 mutations. Phe1434 is found in the middle of the variable loop $L6_c$ and in concert with Met1440 and Phe1443 it contributes to core stabilization (Figures 1B and 4). Its mutation to serine would provide space and a hydrogen bonding partner for neighbouring residues, while introduction of leucine would predominantly modify the hydrophobic interaction pattern. Considering the corresponding 'first site' mutations of Lys1423 it is difficult to rationalize the suppressor effect from presumed direct changes in the interaction patterns. However, the architecture of the $\alpha7_c$/variable loop region shows positions 1423 and 1434 in proximity to each other

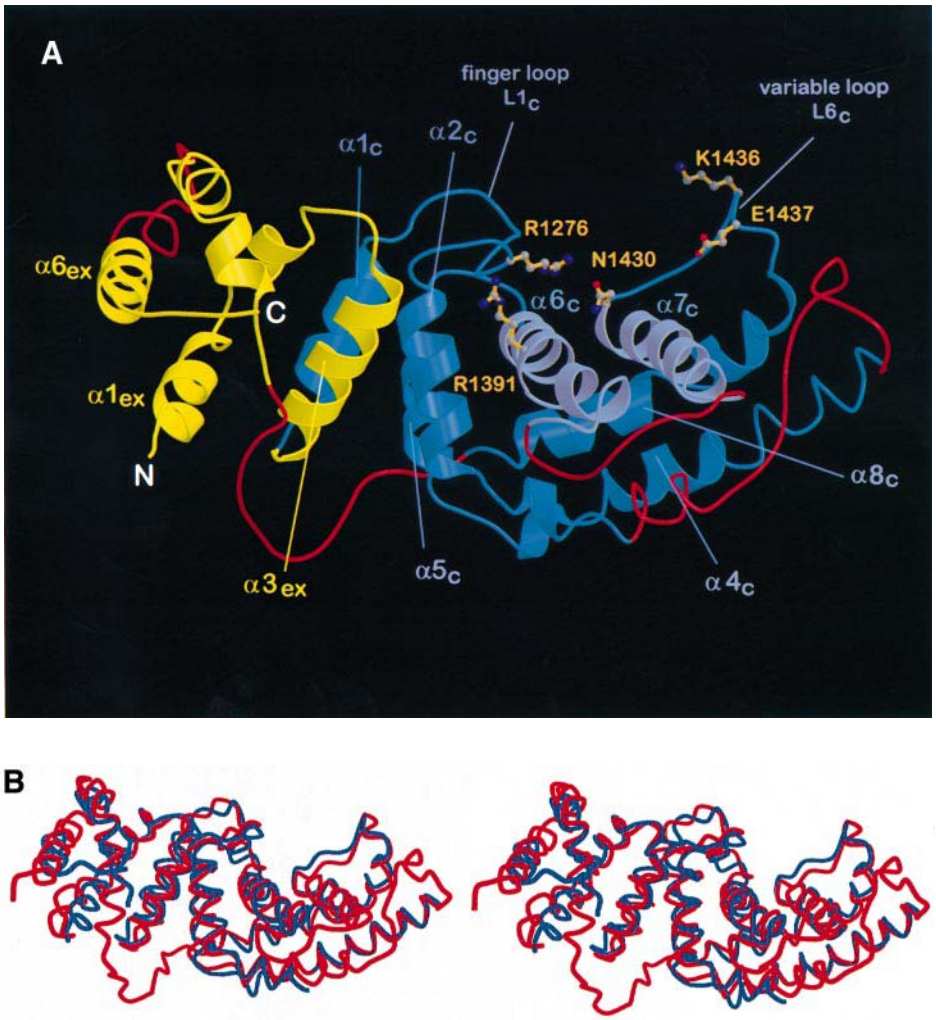

Fig. 2. Structure of NF1-333. (**A**) Ribbon representation of the NF1-333 model. The central domain ($NF1_c$) is in blue and the extra domain ($NF1_{ex}$) in yellow. Regions that are not visible in our model were 'complemented' by the corresponding segments derived from the GAP-334 model and are shown in red (see Figure 2B). Helices $\alpha6_c$ and $\alpha7_c$ forming the bottom of the Ras-binding groove are shown in light blue. Side chains of selected residues presumably involved in polar interactions with Ras (see text) are indicated. K1436 (light grey) appears to be flexible and is modelled stereochemically. (**B**) Structural overlay of NF1-333 (blue) and GAP-334 (red) in stereo representation. (**C**) Sequence alignment of RasGAPs using the models of NF1-333 and GAP-334 as references; assignment of the secondary structure elements is according to the program DSSP (Kabsch and Sander, 1983), thin bars indicate 3_{10} helices, dotted lines regions of high mobility. Abbreviations of species: *hs*, *Homo sapiens*; *sc*, *Saccharomyces cerevisiae*; *bt*, *Bos taurus*; *ss*, *Sus scrofa*; *rn*, *Rattus norvegicus*; *mm*, *Mus musculus*; *ce*, *Caenorhabditis elegans*; *dm*, *Drosophila melanogaster*. The assignment for GAP-334 is based on the final refined model (Table II) deposited with the Protein Data Bank (PDB; accession code 1WER). The minimum catalytic domain (NF230) and the fragment reported by Nur-E-Kamal *et al.* (1993) (NF91) are indicated as are the proteinase K cleavage site (PK) and the location of the type II transcript insertion (21 aa ins) (see Figure 3). The positions of patient mutations are highlighted in yellow. Invariant residues are in red, conserved residues in blue. Amino acids reportedly involved in Ras–RasGAP interaction (Scheffzek *et al*., 1997) are shown in light blue boxes for p120GAP.

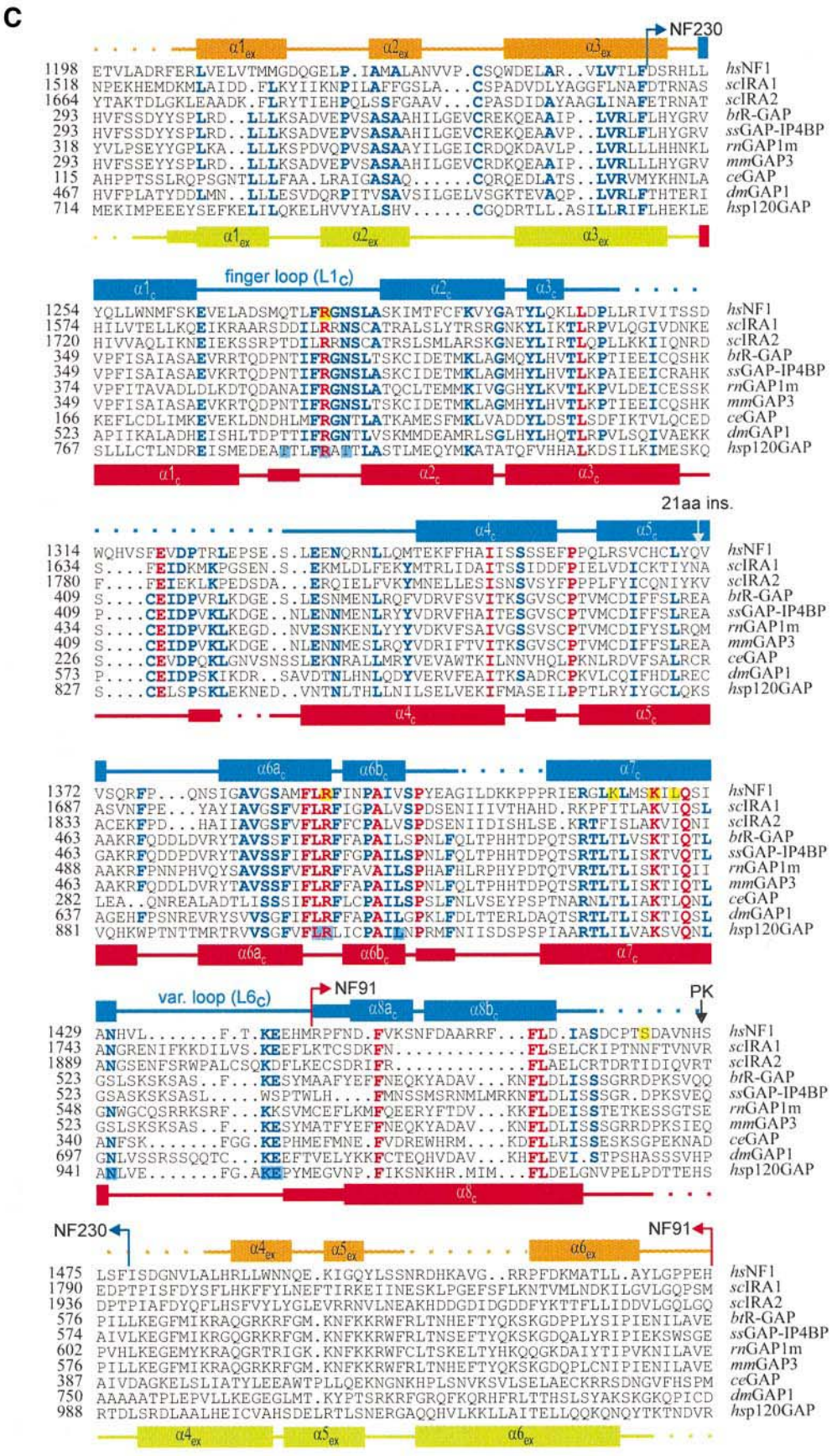
C
NF230
α1ex
α2ex
α3ex
1198 ETVLADRFERLVELVTMMGDQGELP.IAMALANVVP.CSQWDELAR..VLVTLFDSRHLL hsNF1
1518 NPEKHEMDKMLAIDD.FLKYIIKNPILAFFGSLA...CSPADVDLYAGGFLNAFDTRNAS scIRA1
1664 YTAKTDLGKLEAADK.FLRYTIEHPQLSSFGAAV...CPASDIDAYAAGLINAFETRNAT scIRA2
293 HVFSSDYYSPLRD..LLLKSADVEPVSASAAHILGEVCREKQEAAIP..LVRLFLHYGRV btR-GAP
293 HVFSSDYYSPLRD..LLLKSADVEPVSASAAHILGEVCREKQEAAVP..LVRLFLHYGRV ssGAP-IP4BP
318 YVLPSEYYGPLKA..LLLKSPDVQPVSASAAYILGEICRDQKDAVLP..LVRLLLHHNKL rnGAP1m
293 HVFSSEYYSPLRD..LLLKSADVEPVSASAAHILGEVCRDKQEAAIP..LVRLLLHYGRV mmGAP3
115 AHPPTSSLRQPSGNTLLLFAA.LRAIGASAQ......CQRQEDLATS..LVRVMYKHNLA ceGAP
467 HVFPLATYDDLMN..LLLESVDQRPITVSAVSILGELVSGKTEVAQP..LVRLFTHTERI dmGAP1
714 MEKIMPEEEYSEFKELILQKELHVVYALSHV......CGQDRTLL.ASILLRIFLHEKLE hsp120GAP
α1ex
α2ex
α3ex
finger loop (L1C)
α1c
α2c
α3c
1254 YQLLWNMFSKEVELADSMQTLFRGNSLASKIMTFCFKVYGATYLQKLLDPLLRIVITSSD hsNF1
1574 HILVTELLKQEIKRAARSDDILRRNSCATRALSLYTRSRGNKYLIKTLRPVLQGIVDNKE scIRA1
1720 HIVVAQLIKNEIEKSSRPTDILRRNSCATRSLSMLARSKGNEYLIRTLQPLLKKIIQNRD scIRA2
349 VPFISAIASAEVRRTQDPNTIFRGNSLTSKCIDETMKLAGMQYLHVTLKPTIEEICQSHK btR-GAP
349 VPFISAIASAEVKRTQDPNTIFRGNSLASKCIDETMKLAGMHYLHVTLKPAIEEICRAHK ssGAP-IP4BP
374 VPFITAVADLDLKDTQDANAIFRGNSLATQCLTEMMKIVGGHYLKVTLKPVLDEICESSK rnGAP1m
349 VPFISAIASAEVKRTQDPNTIFRGNSLTSKCIDETMKLAGMHYLHVTLKPTIEEICQSHK mmGAP3
166 KEFLCDLIMKEVEKLDNDHLMFRGNTLATKAMESFMKLVADDYLDSTLSDFIKTVLQCED ceGAP
523 APIIKALADHEISHLTDPTTIFRGNTLVSKMMDEAMRLSGLHYLHQTLRPVLSQIVAEKK dmGAP1
767 SLLLCTLNDREISMEDEATTLFRATTLASTLMEQYMKATATQFVHHALKDSILKIMESKQ hsp120GAP
α1c
α2c
α3c
21aa ins.
α4c
α5c
1314 WQHVSFEVDPTRLEPSE.S.LEENQRNLLQMTEKFFHAIISSSSEFPPQLRSVCHCLYQV hsNF1
1634 S....FEIDKMKPGSEN.S..EKMLDLFEKYMTRLIDAITSSIDDFPIELVDICKTIYNA scIRA1
1780 F....FEIEKLKPEDSDA...ERQIELFVKYMNELLESISNSVSYFPPPLFYICQNIYKV scIRA2
409 S....CEIDPVRLKDGE.S.LESNMENLRQFVDRVFSVITKSGVSCPTVMCDIFFSLREA btR-GAP
409 P....CEIDPVKLKDGE..NLENNMENLRYYVDRVFHAITESGVSCPTVMCDIFFSLREA ssGAP-IP4BP
434 S....CEIDPVKLKEGD..NVESNKENLYYYVDKVFSAIVGSSVSCPTVMCDIFYSLRQM rnGAP1m
409 S....CEIDPVKLKDGE..NLENNMESLRQYVDRIFTVITKSGVSCPTVMCDIFFSLREA mmGAP3
226 S....CEVDPQKLGNVSNSSLEKNRALLMRYVEVAWTKILNNVHQLPKNLRDVFSALRCR ceGAP
573 P....CEIDPSKIKDR..SAVDTNLHNLQDYVERVFEAITKSADRCPKVLCQIFHDLREC dmGAP1
827 S....CELSPSKLEKNED..VNTNLTHLLNILSELVEKIFMASEILPPTLRYIYGCLQKS hsp120GAP
α4c
α5c
α6ac
α6bc
α7c
1372 VSQRFP...QNSIGAVGSAMFLRFINPAIVSPYEAGILDKKPPPRIERGLKLMSKILQSI hsNF1
1687 ASVNFPE...YAYIAVGSFVFLRFIGPALVSPDSENIIIVTHAHD.RKPFITLAKVIQSL scIRA1
1833 ACEKFPD...HAIIAVGSFVFLRFFCPALVSPDSENIIDISHLSE.KRTFISLAKVIQNI scIRA2
463 AAKRFQDDLDVRYTAVSSFIFLRFFAPAILSPNLFQLTPHHTDPQTSRTLTLVSKTIQTL btR-GAP
463 GAKRFQDDPDVRYTAVSSFIFLRFFGPAILSPNLFQLTPHHTDPQTSRTLTLISKTVQTL ssGAP-IP4BP
488 AAKRFPNNPHVQYSAVSSFVFLRFFAVAILSPHAFHLRPHYPDTQTVRTLTLISKTIQII rnGAP1m
463 AAKRFQDDLDVRYTAVSSFIFLRFFAPAILSPNLFQLTPHHTDPQTSRTLTLISKTIQTL mmGAP3
282 LEA..QNREALADTLISSSIFLRFLCPAILSPSLFNLVSEYPSPTNARNLTLIAKTLQNL ceGAP
637 AGEHFPSNREVRYSVVSGFIFLRFFAPAILGPKLFDLTTERLDAQTSRTLTLISKTIQSL dmGAP1
881 VQHKWPTNTTMRTRVVSGFVFLRLICPAILNPRMFNIISDSPSPIAARTLILVAKSVQNL hsp120GAP
α6ac
α6bc
α7c
var. loop (L6C)
NF91
PK
α8ac
α8bc
1429 ANHVL.....F.T.KEEHMRPFND.FVKSNFDAARRF...FLD.IASDCPTSDAVNHS hsNF1
1743 ANGRENIFKKDILVS.KEEFLKTCSDKFN.....FLSELCKIPTNNFTVNVR scIRA1
1889 ANGSENFSRWPALCSQKDFLKECSDRIFR.....FLAELCRTDRTIDIQVRT scIRA2
523 GSLSKSKSAS..F...KESYMAAFYEFFNEQKYADAV...KNFLDLISSSGRRDPKSVQQ btR-GAP
523 GSASKSKSASL.....WSPTWLH....FMNSSMSRNMLMRKNFLDLISSSGR.DPKSVEQ ssGAP-IP4BP
548 GNWGCQSRRKSRF...KKSVMCEFLKMFQEERYFTDV...KKFLDEISSTETKESSGTSE rnGAP1m
523 GSLSKSKSAS..F...KESYMATFYEFFNEQKYADAV...KNFLDLISSSGRRDPKSIEQ mmGAP3
340 ANFSK.....FGG.KEPHMEFMNE.FVDREWHRM....KDFLLRISSESKSGPEKNAD ceGAP
697 GNLVSSRSSQQTC...KEEFTVELYKKFCTEQHVDAV...KHFLEVI.STPSHASSSVHP dmGAP1
941 ANLVE.....FG.AKEPYMEGVNP.FIKSNKHR.MIM...FLDELGNVPELPDTTEHS hsp120GAP
α8c
NF230
NF91
α4ex
α5ex
α6ex
1475 LSFISDGNVLALHRLLWNNQE.KIGQYLSSNRDHKAVG..RRPFDKMATLL.AYLGPPEH hsNF1
1790 EDPTPISFDYSFLHKFFYLNEFTIRKEIINESKLPGEFSFLKNTVMLNDKILGVLGQPSM scIRA1
1936 DPTPIAFDYQFLHSFVYLYGLEVRRNVLNEAKHDDGDIDGDDFYKTTFLLIDDVLGQLGQ scIRA2
576 PILLKEGFMIKRAQGRKRFGM.KNFKKRWFRLTNHEFTYQKSKGDPPLYSIPIENILAVE btR-GAP
574 AIVLKEGFMIKRGQGRKRFGM.KNFKKRWFRLTNSEFTYQKSKGDQALYRIPIEKSWSGE ssGAP-IP4BP
602 PVHLKEGEMYKRAQGRTRIGK.KNFKKRWFCLTSKELTYHKQQGKDAIYTIPVKNILAVE rnGAP1m
576 PILLKEGFMIKRAQGRKRFGM.KNFKKRWFRLTNHEFTYQKSKGDQPLCNIPIENILAVE mmGAP3
387 AIVDAGKELSLIATYLEEAWTPLLQEKNGNKHPLSNVKSVLSELAECKRRSDNGVFHSPM ceGAP
750 AAAAATPLEPVLLKEGEGLMT.KYPTSRKRFGRQFKQRHFRLTTHSLSYAKSKGKQPICD dmGAP1
988 RTDLSRDLAALHEICVAHSDELRTLSNERGAQQHVLKKLLAITELLQQKQNQYTKTNDVR hsp120GAP
α4ex
α5ex
α6ex

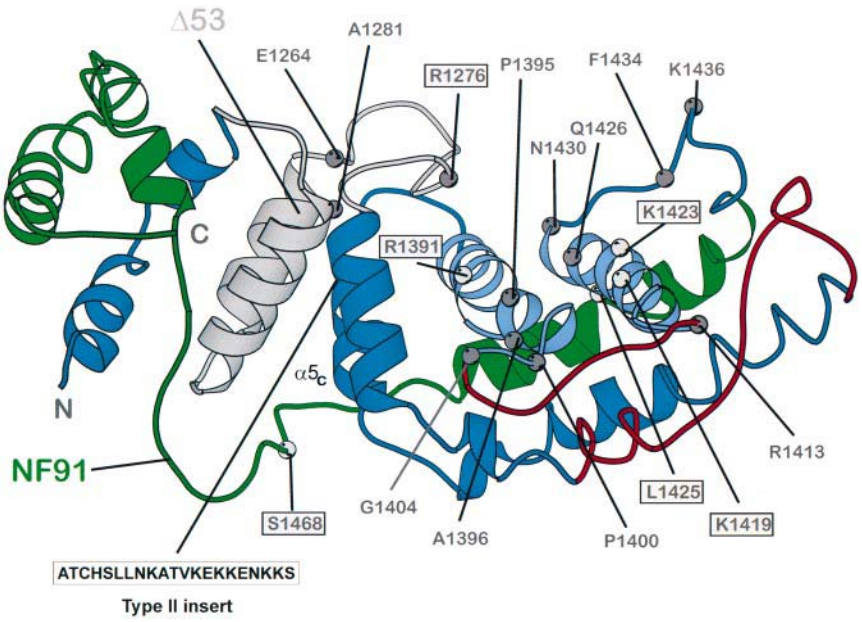

Fig. 3. Sites of NF1GRD mutations. Ribbon drawing of NF1-333 to illustrate the location of mutations found in NF1-patients (light grey spheres, indicated in grey boxes) or derived from mutational analyses (dark grey spheres). The position where 21 amino acids are inserted in the type II transcript is indicated. The extension of the Δ53 deletion (Gutmann *et al*., 1993) is shown in grey, the NF91 fragment reported by Nur-E-Kamal *et al*. (1993) is in green.

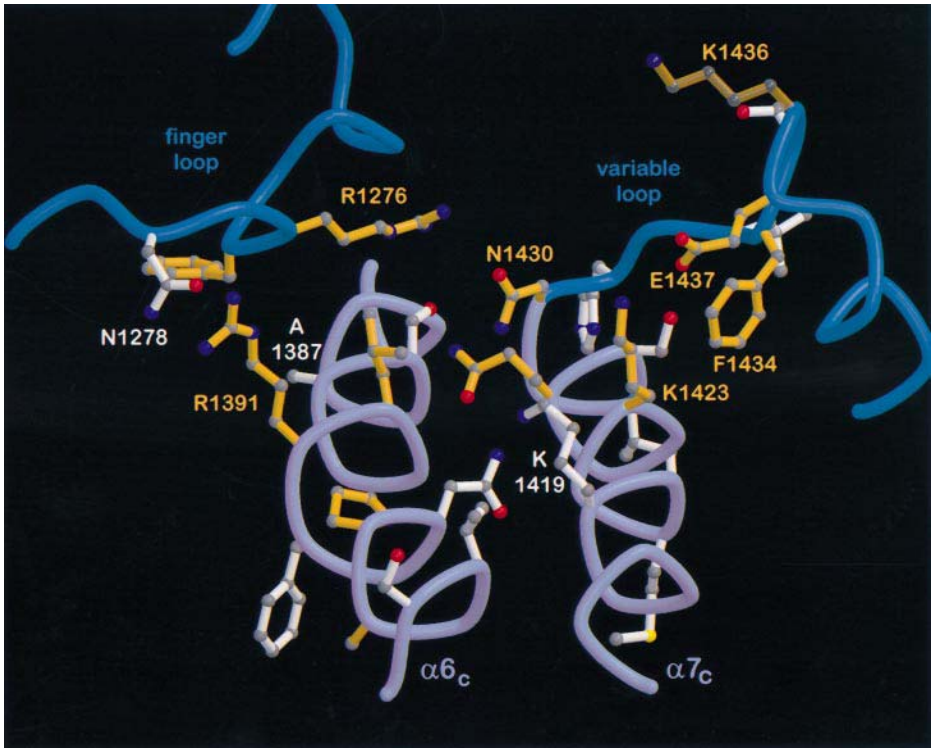

Fig. 4. Details of NF1-333 structure. Segment of NF1-333 showing the putative Ras-binding groove with residues conserved between NF1GRD and GAP-334 shown in orange, and selected amino acids that are different in the two proteins and presumably contribute to differential properties in white. As in Figure 2A, side chain of K1436 is modelled stereochemically.

(Figures 1B and 4) suggesting that they both contribute to the properties of this region that obviously influences the affinity for Ras.

Apart from Lys1423, two other residues located in helix $\alpha 7_c$ were found mutated in NF1 patients, Lys1419 and Leu1425. Sporadic mutations of Lys1419 were found in two cases, once mutated to glutamine (Upadhyaya *et al*., 1997) and to arginine in a patient showing no apparent

malignancy (Purandare *et al*., 1994), with no published biochemical characterization available for either of them. In the structure, Lys1419 protrudes into the surface groove (Figures 1B and 4) and in a hypothetical complex with Ras is in a position to form a salt bridge with Glu37 (see below) from the Ras effector region. Since the corresponding residue in GAP-334 is an isoleucine (Ile931; see above) one might predict that Lys1419 is one of the determinants of neurofibromin's higher affinity for Ras. Leucine 1425 (Klose *et al*., 1998) is in the C-terminal half of helix $\alpha 7_c$ (Figure 3) and mutation to proline would be likely to disrupt the helical geometry of this region, which contains residues Lys1423, Gln1426 and Asn1430, that are all important for successful interaction with Ras.

Serine 1468 is located in a presumed extended chain following $\alpha 8_c$, in a region not visible in our structure. From its location at the C-terminus of $NF1_c$ one would not expect that the mutation to glycine as found in NF1-patients (Upadhyaya *et al*., 1997) interferes with catalysing the GTPase on Ras. Upadhyaya *et al*. (1997) have identified a patient mutation affecting Arg1391 (Arg1391→Ser), that belongs to the FLR-fingerprint motif of RasGAPs. Arg1391 is involved in catalysis (Mittal *et al*., 1996; Ahmadian *et al*., 1997b; Scheffzek *et al*., 1997) and its replacement by serine was shown to reduce GAP activity of neurofibromin 300-fold, although its role in binding and/or catalysis was not differentiated (Upadhyaya *et al*., 1997). The importance of this residue has been recognized in early studies on p120GAP where mutation of Arg903 and Leu902 drastically interfered with GAP function (Brownbridge *et al*., 1993; Skinner *et al*., 1994). Mittal *et al*. (1996) have shown that the Arg1391Met NF1-mutant is no longer able to form a ternary complex with Ras-GDP and aluminium fluoride (AlF_x), the presumed transition state analogue of the GTPase reaction, pointing towards a contribution of this residue in catalysis. Different biochemical effects were observed by Upadhyaya *et al*. (1997), Gutmann *et al*. (1993) and Ahmadian *et al*. (1997b) for Arg1391 mutations, presumably reflecting non-kinetic measurements under different conditions. Under saturating, kinetically controlled conditions the replacement of Arg1391 by alanine decreased the rate of GTP hydrolysis 45-fold (Ahmadian *et al*., 1997b). In the structure of NF1-333, Arg1391 stabilizes the finger loop ($L1_c$) by forming polar interactions with main chain carbonyl oxygens of residues adjacent to Arg1276, the other invariant arginine of RasGAPs, that is even more critical for catalysis (Figure 4; Ahmadian *et al*., 1997b; see below). Shortening the Arg1391 side chain by introducing amino acids other than lysine would disrupt the interaction with the finger loop and thus would be expected to interfere with GAP function.

The substitution Arg1276→Pro was found as an apparently spontaneous mutation in an NF1 patient with a malignant schwannoma (Klose *et al*., 1998). It is the first reported case where a missense mutation in the GRD shows such a particular severe phenotype. The patient had no other alterations in the *NF1* alleles except that the second *NF1* allele is lost, suggesting that the loss of GAP function in this case was the major cause of disease development. Biochemical analysis of the recombinant mutant GRD suggested a structurally intact protein that binds to Ras-GTP but whose GAP activity is reduced 8000-fold, consistent with the finding that in the Ras–RasGAP complex the corresponding residue Arg789 from GAP-334 is in a position to stabilize the transition state of the GTPase reaction, thus being crucial for GAP catalysis (Scheffzek *et al*., 1997). The extremely critical role of this arginine has been demonstrated in another study showing that its replacement by lysine or alanine decreases the reaction rate by three orders of magnitude and abrogates the ability to form a ternary complex with Ras-GDP and AlF_x (Ahmadian *et al*., 1997b). Given the similarity of NF1GRD and GAP-334, Arg1276 can be predicted to contact the nucleotide in a similar way as Arg789 does in the Ras–RasGAP complex.

Site-directed mutagenesis of invariant or conserved residues belonging to different regions of neurofibromin has been carried out by Gutmann *et al*. (1993) (Figure 3). According to the qualitative effects on GAP activity *in vitro* and the ability to suppress heat-shock sensitivity *in vivo*, they were basically grouped into those that behave like wild-type NF1GRD (Pro1395→Ile, Pro1400→Arg, Asn1430→Met), those that showed no activity *in vitro* or *in vivo* (Gln→1426Arg) and those that showed wild-type activity in intact cells but no activity *in vitro* (Glu1264→Tyr, Ala1281→Arg).

Proline 1395 and Pro1400 are located in the C-terminal half of helix $\alpha 6_c$ and according to the Ras–RasGAP structure overlay, substitution by isoleucine or arginine need not necessarily interfere with Ras interaction, as observed by the authors. Asparagine 1430 is located at the C-terminal end of $\alpha 7_c$ (Figures 1B and 4), and the mutation Asn1430→Met has a moderate effect on GAP activity without disturbing the ability to complement GAP function in yeast. A complementary mutation, Asn1430→His, leads to higher Ras affinity, supporting the notion that this residue is involved in, but not crucial for Ras interaction (Morcos *et al*., 1996).

The substitutions Glu1264→Tyr, Ala1281→Arg, Gln1426→Arg and Lys1423→Ser were reported to eliminate GAP activity. Glutamate 1264, the first invariant residue in the GRD-chain, is located at the C-terminal end of helix $\alpha 1_c$ (Figure 3) from where its carboxylate group interacts with the hydroxyl group of Ser1279, which belongs to the finger loop. The mutation to tyrosine might lead to destabilization of the finger-loop region, thereby abrogating GAP activity. Alanine 1281 sits at the N-terminus of helix $\alpha 2_c$ and is buried within a hydrophobic core. Introduction of arginine in this region by the mutation Ala1281→Arg would suggest disruption of structural stability as the major cause for the observed loss of GAP activity. Arginine in the position of Gln1426 (Figures 1B, 3 and 4) is presumably too large to be accommodated in the Ras–NF1GRD interface region.

In the study by Gutmann *et al*. (1993) a deletion (Δ53) spanning residues 1227–1281 was investigated, and complete loss of GAP function reported. Since this segment, which in the structure comprises basically the finger loop with the preceding helices $\alpha 3_{ex}$ and $\alpha 1_c$ (Figure 3), contains the most critical arginine 1276, loss of GAP activity for Δ53 is not surprising. On the other hand, since

removal of at least helix $\alpha 1_c$ is likely to disrupt the protein core one would not even expect Δ53 to form a folded, soluble protein.

A set of mutations was found in a screen for NF1GRD mutants restoring the inability of the yeast Ras-(Asp92→Lys) mutant (Wood *et al*., 1994) to interact with NF1GRD (Morcos *et al*., 1996). Most of these can be mapped to regions that belong to the surface groove of NF1GRD (Figure 3) and some were reported to have high affinity to wild-type Ras as well. These include Arg1413→Gly, Lys1436→Arg, Arg1391→Lys and Arg1276→Gly; Arg1413 belongs to a region that is not well-defined in our structure, therefore the effect of increased affinity cannot be accounted for on the basis of our model. Lysine 1436 together with the subsequent glutamate defines the newly identified KE-motif in Ras-GAPs that is located on the tip of the variable loop (Figures 1B, 3 and 4) (Scheffzek *et al*., 1997). In the complex between Ras and GAP-334 it is in tight contact with an acidic patch presented by the effector loop (Scheffzek *et al*., 1997b). An arginine in this position would allow for even more polar interactions with this region and especially with Asp38, which is in excellent agreement with the increased affinity observed by Mori *et al*. (1995), and as suggested by Nakafuku *et al*. (1993) who showed that this mutant can suppress oncogenic Ras transformation by a mechanism distinct from its GAP activity.

The effect of the increased affinity of the Arg1391→Lys mutant, also observed by Ahmadian *et al*. (1997b), and of Arg1276→Gly cannot be directly rationalized from the structure, but could indicate that the two arginines are not only unnecessary for the ground state of the Ras–RasGAP complex (Geyer *et al*., 1996; Ahmadian *et al*., 1997b), but may actually be inhibitory to it.

Location of the type II transcript insertion

An isoform of neurofibromin resulting from alternative splicing has been found to be expressed in all tissues examined, although the relative amounts vary (Nishi *et al*., 1991; Suzuki *et al*., 1991; Andersen *et al*., 1993). This so-called type II transcript involves the insertion of a 21 amino acid stretch following Gln1370 (Figure 3) and has no counterpart in p120GAP, IRA1 and IRA2. In the structural model an insertion in this position is likely to disrupt the C-terminal part of helix $\alpha 5_c$, and to represent an exposed part of the GRD. From the large number of charged residues (six lysines, two glutamates) clustered in the C-terminal half of the insertion, one might hypothesize that its function involves the interaction with another protein, or maybe even with other regions of neurofibromin itself. Biochemical analyses have detected weaker GAP activity of the type II isoform as compared with type I (Andersen *et al*., 1993), which is due to an apparent weaker binding to Ras (Rey *et al*., 1994). From the structure of NF1GRD and taking into consideration the complex of GAP-334 with Ras, the insertion need not directly interfere with Ras binding, but rather modifies the interaction by long-range electrostatic contributions.

Tubulin binding aspects

Neurofibromin has been found associated with microtubules, suggesting its involvement in microtubule-mediated signal transduction pathways (Gregory *et al*., 1993). Tubulin inhibits GAP activity and the tubulin-binding region appears to overlap with the GRD (Bollag *et al*., 1993). The structure of tubulin and of a bacterial homologue have been determined recently (Loewe *et al*., 1998; Nogales *et al*., 1998), revealing albeit distant similarity to the G-domain fold of Ras (Milburn *et al*., 1990; Pai *et al*., 1990). This supports the observation that Ras and tubulin share common binding sites on their neurofibromin target. Mutations of neurofibromin critical for the interaction with Ras have indeed been shown to affect the interaction with cytoplasmic microtubules as well (Xu and Gutmann, 1997). However, marked differences in the interaction patterns are to be expected, since the tubulin–neurofibromin interaction depends on the presence of 80 residues upstream of NF1-333 (Bollag *et al*., 1993) while the Ras–NF1GRD interaction does not. In the NF1-333 structure (as in GAP-334), N- and C-termini are in proximity to each other (Figure 2A), raising the possibility that residues from both the N- (1095–1198) and C-terminus (1530–1569) of the GRD investigated by Bollag *et al*. (1993) contribute to the architecture of a region critical for tubulin binding.

Implications for the interaction with Ras

The interaction of neurofibromin with Ras has kinetic and thermodynamic characteristics very different from that of p120GAP. This reflects different physiological requirements for this interaction, as demonstrated by the different localization of the two RasGAPs, the different phenotypes of gene knockouts in mice (Brannan *et al*., 1994; Jacks *et al*., 1994; Henkemeyer *et al*., 1995) and *Drosophila* (Gaul *et al*., 1992; The *et al*., 1997), and the fact that neurofibromin but not p120GAP acts as a tumour suppressor in humans. With the structure of NF1GRD and that of the Ras–RasGAP complex represented by Ras-GDP–AlF_3–GAP-334 at hand (Scheffzek *et al*., 1997), we are now able to propose a model for the NF1–Ras interaction by aligning the central domains of NF1GRD and GAP-334 in the Ras–RasGAP complex (Figure 5A). Since the Ras–RasGAP complex was crystallized in the presence of aluminium fluoride, a transition state analogue that is believed to mimic the phosphoryl group transferred during the GTPase reaction (Chabre, 1990; Wittinghofer, 1997), we propose this model to be an albeit rough approximation of the transition state of the NF1GRD accelerated GTPase reaction.

While GTP-hydrolysis rate enhancement by NF1GRD is similar to that by GAP-334, binding affinity for Ras is ~50-fold larger with NF1GRD (Gideon *et al*., 1992; Wiesmüller and Wittinghofer, 1992; Brownbridge *et al*., 1993; Eccleston *et al*., 1993; Ahmadian *et al*., 1997a). Furthermore, both the association and dissociation rate constants for the GAP-334–Ras interaction are too fast to be measured, but can be estimated to be at least 2- and 100-fold faster than the interactions with neurofibromin, respectively. To understand this difference we have investigated the regions of the GAP domains interacting with Ras and screened for differences in amino acid composition. From this comparison we found few amino acids as candidate residues co-responsible for the difference in Ras affinity. Lysine 1419 corresponds to an isoleucine in GAP-334 and is in a position where

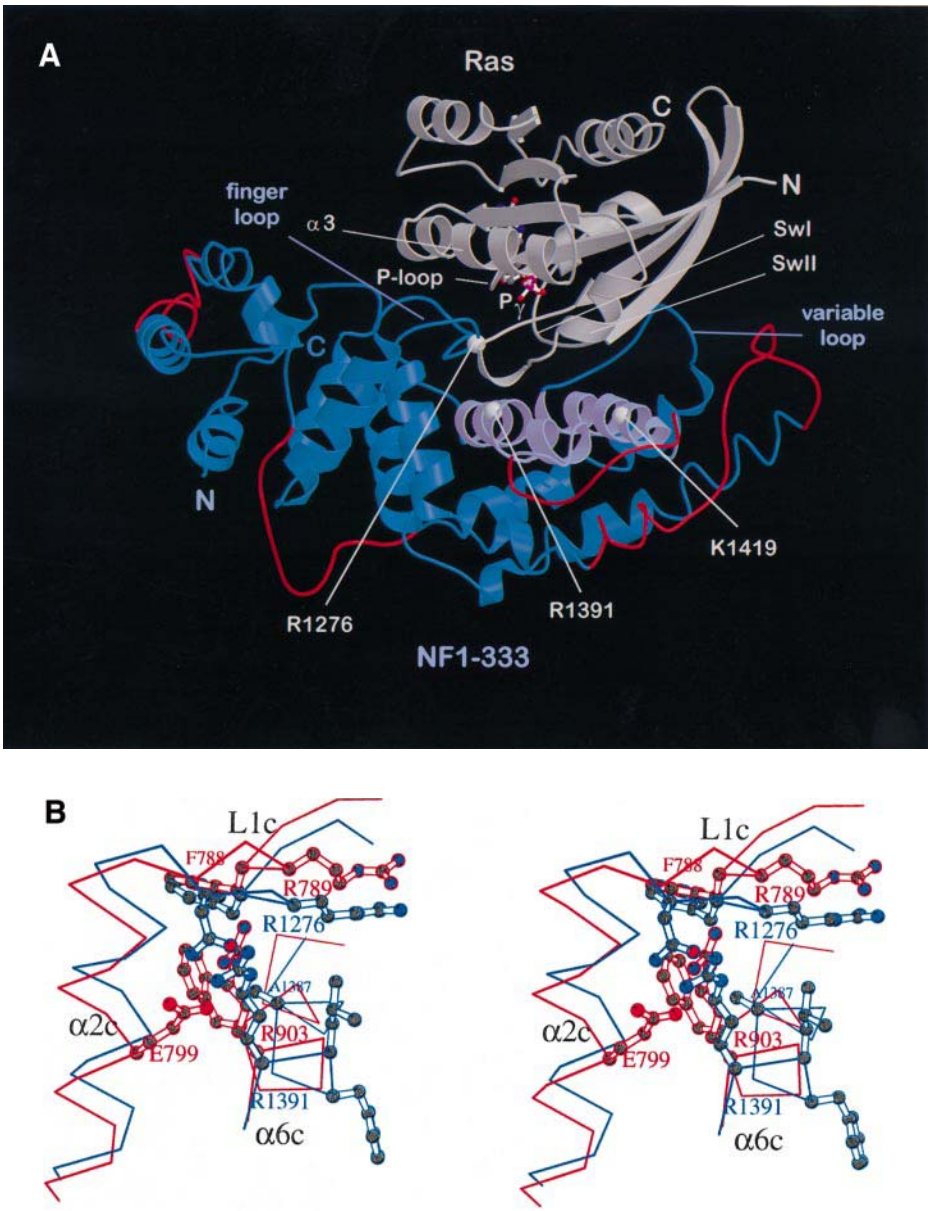

Fig. 5. On the Ras–NF1GRD interaction. (**A**) Hypothetical complex between Ras (grey) and NF1-333 (blue), modelled according to the structure of the Ras-GDP–AlF_3–GAP-334 complex. Segments coloured in red are derived from the GAP-334 model and correspond to regions of presumed high mobility in NF1GRD. SwI, Switch I; SwII, Switch II. Positions of patient mutations affecting the interaction with Ras are indicated by grey spheres. (**B**) Stereo view of the region covering part of a hydrophobic core stabilization of which involves residues derived from the finger loop and from $\alpha 6_c$ (see text).

it might interact with Ras. The proposed Ras–NF1GRD complex would bring Glu37 of the effector region within reach of Lys1419, thus allowing a tight ionic interaction that might contribute to Ras-binding affinity. Another conspicuous difference in the Ras binding groove concerns Thr1286, which corresponds to Glu799 in GAP. In the Ras–RasGAP complex, Glu799 has been pushed aside from its position in uncomplexed GAP-334, making room for the also negatively charged side chain of Glu63 from Ras. In the interaction of Ras with neurofibromin, Thr1286 would be expected to remain in a position to interact with the incoming Glu63.

It has been shown by biochemical and structural analyses that the most important function of GAP is to supply an arginine (the finger) situated on loop $L1_c$ (the finger loop) into the active site of Ras to stabilize the transition state of the GTPase reaction. A striking difference in the finger loop region is Ala790 of GAP-334, which is a glycine in most other RasGAPs including neurofibromin (Figure 2C). With glycine being situated next to the finger arginine (Arg1276), NF1GRD might provide more flexibility to the finger loop and thus allow tighter binding to Ras. Preliminary mutational analysis of this residue (M.Ahmadian, unpublished) supports this idea.

In both NF1GRD and GAP-334, the finger loop is

stabilized by interactions with other regions of the protein, most importantly with the arginine derived from the FLR-motif located in the middle of helix $\alpha 6_c$. We have shown before that this supporting arginine is important in catalysis in that its mutation to alanine reduces the activity of NF1-333 50-fold and abrogates the ability to form a ternary complex with Ras-GDP and AlF_x, whereas mutation to lysine barely affects catalysis (Ahmadian *et al*., 1997b).

In the GAP-334 structure the N-terminal half of helix $\alpha 6_c$ is slightly displaced compared with NF1GRD and appears to be shifted towards the hydrophobic core, stabilizing the helical arrangement. While most of the hydrophobic amino acids located in helix $\alpha 6_c$ are largely similar in NF1GRD and GAP-334, Ala1387 corresponds to a phenylalanine (Phe899) that is tightly involved in core stabilization. It appears that in the absence of the equivalent side chain in NF1GRD, helix $\alpha 6_c$ is less firmly anchored into the core and as a result (Figure 5B) the finger loop might close further down, with Phe1275 becoming more deeply buried within the core. This idea is supported by the observation that in GAP-334 the corresponding Phe788 undergoes hydrophobic interaction with Phe899. As this is one of the most dramatic differences in the amino acid composition we propose it to contribute at least in part to the structural differences in this region and possibly also to differences in the interaction with Ras.

Summarizing the comparison between the Ras–GAP-334 and Ras–NF1 interactions, we can observe that a major difference between the two systems is an increased flexibility of NF1 compared with GAP-334. This might contribute to the slower binding of Ras to NF1GRD, which might need limited conformational adjustments in the latter for tight binding. To compensate for the entropic cost of the conformational change and to explain the higher affinity additional contact points in the interface will be required, although they cannot be inferred from the docking model. Once formed, however, the NF1GRD–Ras complex is much tighter and has a much lower dissociation rate constant.

The difference in binding properties probably reflects the different physiological requirements of the two systems, with Ras localized in the plasma membrane and p120GAP in the cytoplasm, and with the low affinity and low concentration of both proteins it is to be assumed that they can only interact when GAP is relocalized to the plasma membrane during signal transduction. Neurofibromin is localized in the particulate fraction and its high-affinity binding to Ras may allow it to increase GTP hydrolysis without translocation. The knowledge of the structural requirements and the availability of cell lines with the GAP and *NF1* genes disrupted may allow us to test whether engineering GAP to have neurofibromin-like properties and vice versa has any physiological consequences in those cells.

Conclusions

The work reported in this paper characterizes the first functional domain of neurofibromin in three dimensions. In light of the various mutations found in NF1 patients or investigated in structure–function studies, it gives insight into the structure of the GAP-related domain, which in turn may serve as a resource for designing further studies on the function of this protein. Together with the structure of the Ras–RasGAP complex it provides a useful model for analysis of various specific features of NF1GRD–Ras interaction.

Materials and methods

Protein preparation

NF1-333 was expressed as a fusion protein with light meromyosin (LMM) that contained a cleavage site for IgA protease (Ahmadian *et al*., 1996). The fusion protein was purified according to Wolber *et al*. (1992) and cleaved with IgA protease obtained as described (Ahmadian *et al*., 1996). The purified protein was incubated with proteinase K (Boehringer Mannheim) at a substrate to protease ratio of 4000:1 for 60 min and then eluted from a gel filtration column equilibrated with 30 mM Tris–HCl pH 7.5, containing 5 mM $MgCl_2$ and 3 mM DTE. After concentration to 20 mg/ml the protein was stored at –70°C and thawed immediately before setting up crystallization drops. Further analysis was done by mass spectroscopy and polyacrylamide gel electrophoresis, including N-terminal sequencing of blotted bands.

Crystallization

Crystallization was carried out at room temperature by the hanging drop method, where equal amounts (1.5–2 µl) of protein and a solution containing 18–22% poly-ethylene-glycol 3350 (PEG-3350; Sigma), 100 mM Tris–HCl pH 8 and 200 mM $MgCl_2$ were mixed and equilibrated against a reservoir (400 µl) containing the same solution without protein. Crystals appeared after few hours or even minutes and grew within 2–3 days to an average final size of ~600×200×200 µm. Although all preparations resulted in crystallizable protein, high quality crystals as opposed to twinned forms were obtained only by strictly following the preparation protocol. The crystals belong to the monoclinic space group C2 and contain one monomer in the asymmetric unit. They diffract to ~3 Å resolution using a rotating anode, and to better than 2.5 Å in a synchrotron beam.

Data collection and structure determination

Native data were collected using synchrotron radiation (λ = 0.91 Å) on beam line X11 at EMBL Hamburg (c/o DESY). We used the rotation method (oscillation angle, $\Delta\phi$ = 3°) with a MAR image plate detector placed at a crystal-detector distance of 20 cm for data recording. Because of radiation damage and since cryofreezing experiments were not promising, we collected partial data sets from six native crystals altogether, cooled to 4°C. Data processing with the program XDS (Kabsch, 1993) and scaling resulted in a complete merged data set of 2.5 Å resolution (Table I).

Heavy atom derivatives of 12 compounds under various conditions were prepared by soaking crystals in 400 µl of reservoir solution containing 0.1–5 mM of the respective compound. An isomorphous derivative was obtained by treatment of crystals with 0.5 mM methyl mercury chloride (MMCl). A derivative containing K_2PtCl_4 was sufficiently isomorphous when pretreating crystals with MMCl. The effect of MMCl pre-treatment for phasing by this derivative could be improved by instead soaking the crystals in 2 mM iodo acetic acid containing reservoir solution for 24 h before exposure to 0.2 mM K_2PtCl_4, as described above. Derivative data were collected with the rotation method on an area detector (Siemens/Nicolet) mounted before an oscillation camera (Supper; crystal-detector distance, 10 cm; oscillation range, 0.0833°) and a rotating anode (Elliott GX-18; 35 kV/50 mA) with Franks double mirror optics as the X-ray source. Each derivative data set was collected from one single crystal, cooled to ~4°C. Data were processed with XDS (Kabsch, 1993) and analysed with a program suite by W.Kabsch (unpublished; Table I). The solvent-flattened electron density map (Figure 1A), calculated using the phases derived from the heavy atom model, was readily interpretable and required the inversion of the coordinates of heavy atom sites to be consistent with a protein composed of L-amino acids. The GAP-334 model could be accommodated in this map and was used as a guide in subsequent rounds of alternate model building (program 'O'; Jones *et al*., 1991) and refinement with X-PLOR (Version 3.851; Bruenger, 1991), including Powell minimization, simu-

lated annealing, and restrained individual temperature factor refinement. A bulk solvent correction was applied in the final stages of refinement. Graphical representation of the model was done with the programs Molscript (Kraulis, 1991) and Raster3D (Merritt and Bacon, 1997). The Brookhaven Protein Data Bank accession code for the NF1GRD structure is 1NF1.

Acknowledgements

We thank Anna Scherer for skilled technical assistance, Hans Wagner for excellent maintenance of the X-ray facilities at the Max-Planck-Institut für medizinische Forschung (Heidelberg), Alfred Lautwein, Andreas Becker, Werner Jahn and Ingrid Vetter for helpful discussions, Friedhelm Dräger for help with Figure 2B, Rita Schebaum for secretarial assistance and Ken Holmes for general support. We thank Victor Lamzin and Paul Tucker at EMBL Hamburg (c/o DESY) for advice during data collection and Arnon Lavie for sharing beam time. K.S. gratefully acknowledges support by the Peter and Traudl Engelhorn Stiftung (Penzberg, Germany) and by the National Neurofibromatosis Foundation (New York, USA), and A.W. the support of the EU (Bio4CT, 961110).

References

Ahmadian,M.R., Wiesmüller,L., Lautwein,A., Bischoff,F.R. and Wittinghofer,A. (1996) Structural differences in the minimal catalytic domains of the GTPase-activating proteins $p120^{GAP}$ and Neurofibromin. *J. Biol. Chem*., **271**, 16409–16415.

Ahmadian,M.R., Hoffmann,U., Goody,R.S. and Wittinghofer,A. (1997a) Individual rate constants for the interaction of Ras proteins with GTPase-activating proteins determined by fluorescence spectroscopy. *Biochemistry*, **36**, 4535–4541.

Ahmadian,M.R., Stege,P., Scheffzek,K. and Wittinghofer,A. (1997b) Confirmation of the arginine-finger hypothesis for the GAP-stimulated GTP-hydrolysis reaction of Ras. *Nature Struct. Biol.*, **4**, 686–689.

Andersen,L.B., Ballester,R., Marchuk,D.A., Chang,E., Gutman,D.H., Saulino,A.M., Camonis,J., Wigler,M. and Collins,F.S. (1993) A conserved alternative splice in the von Recklinghausen neurofibromatosis (NF1) gene produces two neurofibromin isoforms, both of which have GTPase-activating protein activity. *Mol. Cell. Biol*., **13**, 487–495.

Bader,J.L. (1986) Neurofibromatosis and cancer. *Ann. NY Acad. Sci*., **486**, 57–65.

Ballester,R., Marchuk,D., Boguski,M., Saulino,A., Letcher,R., Wigler,M. and Collins,F. (1990) The *NF1* locus encodes a protein functionally related to mammalian GAP and yeast IRA proteins. *Cell*, **63**, 851–859.

Basu,T.N., Gutmann,D.H., Fletcher,J.A., Glover,T.W., Collins,F.S. and Downward,J. (1992) Aberrant regulation of ras proteins in malignant cells from type 1 neurofibromatosis patients. *Nature*, **356**, 713–715.

Bollag,G. and McCormick,F. (1991) Differential regulation of rasGAP and neurofibromatosis gene product activities. *Nature*, **351**, 576–579.

Bollag,G., McCormick,F. and Clark,R. (1993) Characterization of full-length neurofibromin: tubulin inhibits ras GAP activity. *EMBO J.*, **12**, 1923–1927.

Brannan,C.I. *et al.* (1994) Targeted disruption of the neurofibromatosis type-1 gene leads to developmental abnormalities in heart and various neural crest-derived tissues. *Genes Dev.*, **8**, 1019–1029.

Brownbridge,G.G., Lowe,P.N., Moore,K.J.M., Skinners,R.H. and Webb,M.R. (1993) Interaction of GTPase activating proteins (GAPs) with $p21^{ras}$ measured by a novel fluorescence anisotropy method. *J. Biol. Chem*., **268**, 10914–10919.

Bruenger,A.T. (1991) X-PLOR, a system for crystallography and NMR. Yale University, New Haven, CT.

Cawthon,R.M. *et al.* (1990) A major segment of the neurofibromatosis type 1 gene: cDNA sequence, genomic structure and point mutations. *Cell*, **62**, 193–201.

Chabre,M. (1990) Aluminofluoride and beryllofluoride complexes: new phosphate analogs in enzymology. *Trends Biochem. Sci.*, **15**, 6–10.

DeClue,J.E., Cohen,B.D. and Lowy,D.R. (1991) Identification and characterization of the neurofibromatosis type 1 protein product. *Proc. Natl Acad. Sci. USA*, **88**, 9914–9918.

DeClue,J.E., Papageorge,A.G., Fletcher,J.A., Diehl,S.R., Ratner,N., Vass,W.C. and Lowy,D.R. (1992) Abnormal regulation of mammalian $p21^{ras}$ contributes to malignant tumour growth in von Recklinghausen (type 1) neurofibromatosis. *Cell*, **69**, 265–273.

Eccleston,J.F., Moore,K.J.M., Morgan,L., Skinner,R.H. and Lowe,P.N. (1993) Kinetics of interaction between normal and proline 12 Ras and the GTPase-activating proteins, p120-GAP and neurofibromin. *J. Biol. Chem.*, **268**, 27012–27019.

Fridman,M. *et al*. (1994) The minimal fragments of c-Raf-1 and NF1 that can suppress v-Ha-Ras-induced malignant phenotype. *J. Biol. Chem.*, **269**, 30105–30108.

Gaul,U., Mardon,G. and Rubin,G.M. (1992) A putative ras GTPase activating protein acts as a negative regulator of signalling by the Sevenless receptor tyrosine kinase. *Cell*, **68**, 1007–1019.

Geyer,M., Schweins,T., Herrmann,C., Prisner,T., Wittinghofer,A. and Kalbitzer,H.R. (1996) Conformational transitions in free $p21^{H\text{-}ras}$ and in $p21^{H\text{-}ras}$ complexed with the effector protein Raf-RBD and the GTPase activating protein GAP. *Biochemistry*, **35**, 10308–10320.

Gideon,P., John,J., Frech,M., Lautwein,A., Clark,R., Scheffler,J.E. and Wittinghofer,A. (1992) Mutational and kinetic analysis of the GTPase-activating protein (GAP)-p21 interaction: The C-terminal domain of GAP is not sufficient for full activity. *Mol. Cell. Biol.*, **12**, 2050–2056.

Golubic,M., Tanaka,K., Dobrowolski,S., Wood,D., Tsai,M.H., Marshall,M., Tamanoi,F. and Stacey,D.W. (1991) The GTPase stimulatory activities of the neurofibromatosis gene type 1 and the yeast IRA2 proteins are inhibited by arachidonic acid. *EMBO J.*, **10**, 2897–2903.

Gregory,P.E., Gutmann,D.H., Mitchell,A., Park,S., Boguski,M., Jacks,T., Wood,D.L., Jove,R. and Collins,F.S. (1993) Neurofibromatosis type 1 gene product (Neurofibromin) associates with microtubules. *Somat. Cell Mol. Genet.*, **19**, 265–274.

Griesser,J., Kaufmann,D., Eisenbarth,I., Bäuerle,C. and Krone,W. (1995) Ras-GTP regulation is not altered in cultured melanocytes with reduced levels of neurofibromin derived from patients with neurofibromatosis 1 (NF1). *Biol. Chem. Hoppe-Seyler*, **376**, 91–101.

Guha,A., Lau,N., Huvar,I., Gutmann,D., Provias,J., Pawson,T. and Boss,G. (1996) Ras-GTP levels are elevated in human NF1 peripheral nerve tumors. *Oncogene*, **12**, 507–513.

Gutmann,D.H. and Collins,F.S. (1993) The neurofibromatosis type 1 gene and its protein product, Neurofibromin. *Neuron*, **10**, 335–343.

Gutmann,D.H., Boguski,M., Marchuk,D., Wigler,M., Collins,F.S. and Ballester,R. (1993) Analysis of the neurofibromatosis type 1 (NF1) GAP-related domain by site-directed mutagenesis. *Oncogene*, **8**, 761–769.

Gutmann,D.H., Geist,R.T., Rose,K. and Wright,D.E. (1995) Expression of two new protein isoforms of the neurofibromatosis type 1 gene product, neurofibromin, in muscle tissues. *Dev. Dyn.*, **202**, 302–311.

Henkemeyer,M., Rossi,D.J., Holmyard,D.P., Puri,M.C., Mbamalu,G., Harpal,K., Shih,T.S., Jacks,T. and Pawson,T. (1995) Vascular system defects and neuronal apoptosis in mice lacking Ras GTPase-activating protein. *Nature*, **377**, 695–701.

Jacks,T., Shi,T.S., Schmitt,E.M., Bronson,R.T., Bernards,A. and Weinberg,R. (1994) Tumour predisposition in mice heterozygous for a targeted mutation in Nf1. *Nature Genet.*, **7**, 353–361.

Johnson,M.R., DeClue,J.E., Felzmann,S., Vass,W.C., Xu,G., White,R. and Lowy,D.R. (1994) Neurofibromin can inhibit ras-dependent growth by a mechanism independent of its GTPase-accelerating function. *Mol. Cell. Biol*., **14**, 641–645.

Jones,T.A., Zou,J.Y., Cowan,S.W. and Kjelgaard,M. (1991) Improved methods for building protein models in electron density maps and the location of errors in these models. *Acta Crystallogr.*, **A47**, 110–119.

Kabsch,W. (1993) Automatic processing of rotation diffraction data from crystal of initially unknown symmetry and cell constants. *J. Appl. Crystallogr.*, **26**, 795–800.

Kabsch,W. and Sander,C. (1983) Dictionary of protein secondary structures: pattern recognition of hydrogen-bonded and geometrical features. *Biopolymers*, **22**, 2577–2637.

Klose,A.J. *et al*. (1998) Selective disactivation of neurofibromin GAP-activity in neurofibromatosis type 1 (NF1). *Hum. Mol. Genet*., **7**, 1261–1268.

Kraulis,P. (1991) Molscript: a program to produce both detailed and schematic protein structures. *J. Appl. Crystallogr.*, **24**, 946–950.

Li,Y. *et al.* (1992) Somatic mutations in the neurofibromatosis 1 gene in human tumors. *Cell*, **69**, 275–281.

Loewe,J. and Amos,L.A. (1998) Crystal structure of the bacterial cell-division protein FtsZ. *Nature*, **391**, 203–206.

Lowy,D.R. and Willumsen,B.M. (1993) Function and regulation of Ras. *Annu. Rev. Biochem.*, **62**, 851–891.

Marchuk,D.A. *et al.* (1991) cDNA cloning of the type 1 neurofibromatosis gene: complete sequence of the *NF1* gene product. *Genomics*, **11**, 931–940.

Marshall,M.S., Hill,W.S., Ng,A.S., Vogel,U.S., Schaber,M.D., Scolnick, E.M., Dixon,R.A.F., Sigal,I. and Gibbs,J.B. (1989) A C-terminal domain of GAP is sufficient to stimulate ras p21 GTPase activity. *EMBO J*., **8**, 1105–1110.

Martin,G.A. *et al.* (1990) The GAP-related domain of the neurofibromatosis type 1 gene product interacts with *ras* p21. *Cell*, **63**, 843–849.

Merrit,E.A. and Bacon,D.J. (1997) Raster3D: Photorealistic molecular graphics. *Methods Enzymol.*, **277**, 505–524.

Milburn,M.V., Tong,L., DeVos,A.M., Brünger,A., Yamaizumi,Z., Nishimura,S. and Kim,S.-H. (1990) Molecular switch for signal transduction: structural differences between active and inactive forms of protooncogenic *ras* proteins. *Science*, **247**, 939–945.

Mittal,R., Ahmadian,M.R., Goody,R.S. and Wittinghofer,A. (1996) Formation of a transition state analog of the Ras GTPase reaction by Ras•GDP, tetrafluoroaluminate and GTPase-activating proteins. *Science*, **273**, 115–117.

Morcos,P., Thapar,N., Tusneem,N., Stacey,D. and Tamanoi,F. (1996) Identification of neurofibromin mutants that exhibit allele specificity or increased Ras affinity resulting in suppression of activated *ras* alleles. *Mol. Cell. Biol*., **16**, 2496–2503.

Mori,S., Satoh,T., Koide,H., Nakafuku,M., Villafranca,E. and Kaziro,Y. (1995) Inhibition of Ras/Raf interaction by anti-oncogenic mutants of neurofibromin, the neurofibromatosis type 1 (NF1) gene product, in cell-free systems. *J. Biol. Chem*., **270**, 28834–28838.

Nakafuku,M., Nagamine,M., Ohtoshi,A., Tanaka,K., Toh-E,A. and Kaziro,Y. (1993) Suppression of oncogenic Ras by mutant neurofibromatosis type 1 genes with single amino acid substitutions. *Proc. Natl Acad. Sci. USA*, **90**, 6706–6710.

Nishi,T., Lee,P.S.Y., Oka,K., Levin,V.A., Tanase,S., Morino,Y. and Saya,H. (1991) Differential expression of two types of the neurofibromatosis type 1 (*NF1*) gene transcripts related to neuronal differentiation. *Oncogene*, **6**, 1555–1559.

Nixon,A.E., Brune,M., Lowe,P.N. and Webb,M. (1995) Kinetics of inorganic phosphate release during the interaction of $p21^{ras}$ with the GTPase-activating proteins p120-GAP and neurofibromin. *Biochemistry*, **34**, 15592–15598.

Nogales,E., Wolf,S.G. and Downing,K.H. (1998) Structure of the αβ tubulin dimer by electron crystallography. *Nature*, **391**, 199–203.

Nur-E-Kamal,M.S.A., Varga,M. and Maruta,H. (1993) The GTPase-activating NF1 fragment of 91 amino acids reverses v-Ha-Ras-induced malignant phenotype. *J. Biol. Chem*., **268**, 22331–22337.

Pai,E.F., Krengel,U., Petsko,G.A., Goody,R.S., Kabsch,W. and Wittinghofer,A. (1990) Refined crystal structure of the triphosphate conformation of H-ras p21 at 1.35 Å resolution: implications for the mechanism of GTP hydrolysis. *EMBO J*., **9**, 2351–2359.

Ponder,B.A.J. (1990) Inherited predisposition to cancer. *Trends Genet*., **6**, 213–218.

Poullet,P., Lin,B., Esson,K. and Tamanoi,F. (1994) Functional significance of lysine 1423 of neurofibromin and characterization of a second site suppressor which rescues mutations at this residue and suppresses $RAS2^{Val\text{-}19}$-activated phenotypes. *Mol. Cell. Biol*., **14**, 815–821.

Purandare,S.M., Lanyon,W.G. and Connor,J.M. (1994) Characterisation of inherited and sporadic mutations in neurofibromatosis type-1. *Hum. Mol. Genet.*, **3**, 1109–1115.

Rey,I., Taylor-Harris,P., van Erp,H. and Hall,A. (1994) R-ras interacts with rasGAP, neurofibromin and c-raf but does not regulate cell growth or differentiation. *Oncogene*, **9**, 685–692.

Riccardi,V.M. (1981) Von Recklinghausen neurofibromatosis. *N. Engl. J. Med.*, **305**, 1617–1627.

Riccardi,V.M. (1991) Neurofibromatosis: past, present and future. *N. Engl. J. Med*., **324**, 1283–1285.

Riccardi,V.M. and Eichner,J.E. (1986) *Neurofibromatosis: Phenotype, Natural History and Pathogenesis*. Johns Hopkins University Press, Baltimore, MD, USA.

Scheffzek,K., Lautwein,A., Kabsch,W., Ahmadian,M.R. and Wittinghofer,A. (1996) Crystal structure of the GTPase-activating domain of human p120GAP and implications for the interaction with Ras. *Nature*, **384**, 591–596.

Scheffzek,K., Ahmadian,M.R., Kabsch,W., Wiesmüller,L., Lautwein,A., Schmitz,F. and Wittinghofer,A. (1997) The Ras–RasGAP complex: Structural basis for GTPase activation and its loss in oncogenic Ras mutants. *Science*, **277**, 333–338.

Serra,E., Puig,S., Otero,D., Gaona,A., Kruyer,H., Ars,E., Estivill,X. and Lázaro,C. (1997) Confirmation of a double-hit model for the NF1 gene in benign neurofibromas. *Am. J. Hum. Genet.*, **61**, 512–519.

Serth,J., Lautwein,A., Frech,M., Wittinghofer,A. and Pingoud,A. (1991) The inhibition of the GTPase activating protein–Ha-ras interaction by acidic lipids is due to physical association of the C-terminal domain of the GTPase activating protein with micellar structures. *EMBO J*., **10**, 1325–1330.

Shen,M.H., Harper,P.S. and Upadhyaya,M. (1996) Molecular genetics of neurofibromatosis type 1 (NF1). *J. Med. Genet.*, **33**, 2–17.

Skinner,R.H., Picardo,M., Gane,N.M., Cook,N.D., Morgan,L., Rowedder,J. and Lowe,P.N. (1994) Direct measurement of the binding of RAS to neurofibromin using a scintillation proximity assay. *Anal. Biochem.*, **223**, 259–265.

Stanbridge,E.J. (1990) Human tumor suppressor genes. *Annu. Rev. Genet*., **24**, 615–657.

Suzuki,Y., Suzuki,H., Kayama,T., Yoshimoto,T. and Shibahara,S. (1991) Brain tumors predominantly express the neurofibromatosis type 1 gene transcripts containing the 63 base insert in the region coding for GTPase activating protein-related domain. *Biochem. Biophys. Res. Commun.*, **181**, 955–961.

Tanaka,K., Nakafuku,M., Satoh,T., Marshall,M.S., Gibbs,J.B., Matsumoto,K., Kaziro,Y. and Toh-e,A. (1990a) *S.cerevisiae* genes *IRA1* and *IRA2* encode proteins that may be functionally equivalent to mammalian ras GTPase activating protein. *Cell*, **60**, 803–807.

Tanaka,K., Nakafuku,M., Tamanoi,F., Kaziro,Y., Matsumoto,K. and Tohe,A. (1990b) *IRA2*, a second gene of *Saccharomyces cerevisiae* that encodes a protein with a domain homologous to mammalian *ras* GTPase-activating protein. *Mol. Cell. Biol.*, **10**, 4303–4313.

Tanaka,K., Lin,B.K., Wood,D.R. and Tamanoi,F. (1991) IRA2, an upstream negative regulator of RAS in yeast, is a RAS GTPase-activating protein. *Proc. Natl Acad. Sci. USA*, **88**, 468–472.

The,I., Hannigan,G.E., Cowley,G.S., Reginald,S., Zhong,Y., Gusella,J.F., Hariharan,I.K. and Bernards,A. (1997) Rescue of a *Drosophila* NF1 mutant phenotype by protein kinase A. *Science*, **276**, 791–794.

Trahey,M. and McCormick,F. (1987) A cytoplasmic protein stimulates normal N-ras p21 GTPase, but does not affect oncogenic mutants. *Science*, **238**, 542–545.

Tsai,M.-H., Roudebush,M., Dobrowolski,S., Yu,C.-L., Gibbs,J.B. and Stacey,D.W. (1991) Ras GTPase-activating protein physically associates with mitogenically active phospholipids. *Mol. Cell. Biol*., **11**, 2785–2793.

Upadhyaya,M., Osborn,M.J., Maynard,J., Kim,M.R., Tamanoi,F. and Cooper,D.N. (1997) Mutational and functional analysis of the neurofibromatosis type 1 (*NF1*) gene. *Hum. Genet.*, **99**, 88–92.

Viskochil,D. *et al.* (1990) Deletions and a translocation interrupt a cloned gene at the neurofibromatosis type 1 locus. *Cell*, **62**, 187–192.

Wallace,M.R. *et al.* (1990) Type 1 neurofibromatosis gene: identification of a large transcript disrupted in three NF1 patients. *Science*, **249**, 181–186.

Wiesmüller,L. and Wittinghofer,A. (1992) Expression of the GTPase activating domain of the neurofibromatosis type 1 (*NF1*) gene in *E.coli* and role of the conserved lysine residue. *J. Biol. Chem*., **267**, 10207–10210.

Wittinghofer,A. (1997) Signaling mechanistics: Aluminum fluoride for molecule of the year. *Curr. Biol.*, **7**, R682–R685.

Wolber,V., Maeda,K., Schumann,R., Brandmeier,B., Wiesmüller,L. and

Wittinghofer,A. (1992) A universal expression-purification system based on the coiled-coil interaction of myosin heavy chain. *Biotechnology*, **10**, 900–904.

Wood,D.R., Poullet,P., Wilson,B.A., Khalil,M., Tanaka,K., Cannon,J.F. and Tamanoi,F. (1994) Biochemical characterization of yeast *RAS2* mutants reveals a new region of ras protein involved in the interaction with GTPase-activating proteins. *J. Biol. Chem*., **269**, 5322–5327.

Xu,G. *et al.* (1990a) The neurofibromatosis type 1 gene encodes a protein related to GAP. *Cell*, **62**, 599–608.

Xu,G.F., Lin,B., Tanaka,K., Dunn,D., Wod,D., Gesteland,R., White,R., Weiss,R. and Tamanoi,F. (1990b) The catalytic domain of the neurofibromatosis type 1 gene product stimulates ras GTPase and complements ira mutants of *S.cerevisiae. Cell*, **63**, 835–841.

Xu,H. and Gutmann,D.H. (1997) Mutations in the GAP-related domain impair the ability of neurofibromin to associate with microtubules. *Brain Res.*, **759**, 149–152.

Received March 30, 1998; revised May 29, 1998; accepted June 2, 1998